Environmental Research 229 (2023) 115976

Contents lists available at ScienceDirect

Environmental Research

journal homepage: www.elsevier.com/locate/envres

Thermal plasma potential to remediate soil contaminated with diesel☆

Dovilė Gimžauskaitė *, Andrius Tamošiūnas, Mindaugas Aikas, Rolandas Uscila

Lithuanian Energy Institute, Plasma Processing Laboratory, Breslaujos str. 3, LT-44403 Kaunas, Lithuania

ARTICLE INFO

Keywords:
Soil de-pollution
Petroleum hydrocarbons (PHCs)
Diesel
Thermal plasma
Producer gas

ABSTRACT

Petroleum hydrocarbons (PHCs) are recognized as one of the major soil contaminants causing negative environmental impact. Thereby, PHCs remediation from the soil is essential. Hence, this experimental study aimed to assess the potential of thermal water vapor and air plasmas to remediate soil contaminated with habitually used PHCs – diesel. The impact of contaminant content in the soil on the remediation process also was estimated. The results of this research demonstrated that 99.9% contaminant removal efficiency was received proceeding diesel contaminated soil remediation in the environment of the thermal plasma in defiance of whether water vapor or air was employed as a plasma-forming gas. Moreover, the soil's contaminant content (80–160 g/kg) did not influence its' removal efficiency. The soil de-pollution process also caused the decomposition of the soils' natural carbon reserves since carbon content decreased from an initial 9.8 wt% in the clean soil to 3–6 wt% in the remediated soil. Furthermore, PHCs – diesel was decomposed into producer gas mainly consisting of H_2, CO (also known as synthesis gas) and CO_2. Thus, the thermal plasma offers a way not only to de-pollute the soil but also to reuse the PHCs present in the soil by breaking it down into gaseous products that can further be used to meet human needs.

1. Introduction

The increasing global population, which induces the ever-increasing necessity for goods and constantly growing industrialization, ineluctably causes contamination of the natural environment, including water, air, and soil, an essential component of human and other living beings' existence (Aggelopoulos, 2022; Azhar et al., 2022; Liu et al., 2023). According to FAO and UNEP, in order of importance, the main sources of the basic contaminants causing soil pollution are industrial activities, mining, waste treatment, agriculture, fossil fuels extraction and processing, and transport emissions. However, there is a lack of specific, reliable, and compatible statistics on the actual emissions of each sector (FAO and UNEP, 2021). Focusing on petroleum-derived fuels, the main sources of soil contamination with petroleum hydrocarbons (PHCs) are petroleum production, petrochemical industries, vehicle exhaust, waste engine oil, petroleum sludge, and oil spills. Hence, leakages from storage tanks, accidental spills, and improper disposal are well-known ways of releasing PHCs (crude oil, jet range fuels, diesel, gasoline) into the environment (Ambaye et al., 2022; Hidalgo et al., 2020; Murphy et al., 2022). PHCs are organic compounds consisting mainly of carbon and hydrogen atoms arranged in differing structural configurations encompassing alkanes, cycloalkanes, and polycyclic aromatic hydrocarbons. Pyrene, benzene, naphthalene, cyclohexane, butane, pentane, and cyclopentene are known as one of toxic petroleum hydrocarbons that could be found in contaminated soil. Although petroleum hydrocarbons mainly comprise carbon and hydrogen, they also contain small amounts of sulfur, nitrogen, and oxygen (Ambaye et al., 2022; Gkorezis et al., 2016; Haider et al., 2021). Amongst petroleum hydrocarbons, diesel is one of the most frequently used PCHs nowadays, which mainly consists of recalcitrant and less biodegradable hydrocarbons with 8–28 carbon atoms, including alkanes, cycloalkanes and polycyclic aromatic hydrocarbons (Liu et al., 2022a; Shang et al., 2023; Wong et al., 2022). Moreover, diesel and other PHCs have high hydrophobic properties and show stability and longevity in the soil environment. Thus, the low diesel water solubility impedes diesel's easy removal from the soil. Generally, diesel and other PHCs accumulate on the soil's surface, fill soil pores, and create the soil aggregation effect due to diesel non-polarity, allowing diesel to bond with organic matter present in the soil. Consequently, this combination between diesel and soil creates water, oxygen, and vital nutrients, such as nitrogen and phosphorous shortages in the soil. Also, diesel contamination creates a damaging, toxicological effect not only on the soil environment but also on groundwater and

☆ Declaration of interests.

* Corresponding author.
E-mail address: Dovile.Gimzauskaite@lei.lt (D. Gimžauskaitė).

https://doi.org/10.1016/j.envres.2023.115976
Received 1 March 2023; Received in revised form 16 April 2023; Accepted 21 April 2023
Available online 22 April 2023

surrounding water, as well as human and animal well-being (Das et al., 2022; Haider et al., 2021; C.Liu et al., 2022a; F.Liu et al., 2022b; Priyadarshini and Chattopadhyay, 2022). Therefore, the damaging effect of diesel and other PHCs on the environment encourages researchers to look for efficient soil de-pollution methods capable of remediating diesel and other organic contaminants from the soil. In this context, diverse physical, chemical, biological, and thermochemical methods are used for soil remediation. These methods are broadly described here: (Ambaye et al., 2022; Dai et al., 2022; Lv et al., 2022; Mambwe et al., 2021; Ossai et al., 2020). Meanwhile, this paper focuses on applying the plasma-based method for contaminated soil de-pollution. Plasma treatment has recently become recognized as an alternative thermochemical method for the remediation of soil polluted with organic contaminants. Organic materials in the plasma environment can be decomposed into a beneficial intermediate product called synthesis gas. Also, plasma technologies are distinguished by the fact that their application does not require the use of supplementary chemical materials or often costly catalysts. Another vital advantage of this technology is the fast-cleaning time since rich with reactive species plasma environment warrants efficient chemical reactions (Gimžauskaitė et al., 2022; Rahman et al., 2015). Moreover, recently Sanjaya et al. (Sanjaya and Abbas, 2023) evaluated plasma gasification according to the life cycle assessment aspect. The authors' analysis showed the plasma gasification environmental superiority over Energy-from-Waste technologies (e.g., traditional gasification, landfilling, etc.) and has demonstrated its alignment with the circular economy principle: circulating materials and products at their highest value with minimum impact on the environment.

Furthermore, focusing on soil remediation, non-thermal plasma technologies are frequently applied to de-pollute soil contaminated with organic compounds. Additionally, the novelty and scientific innovation of the present work lies within the fact that thermal plasma is frequently applied for various waste or biomass gasification. Nevertheless, to the authors' knowledge, there is a lack of articles investigating the potential to use thermal plasma to de-pollute soil contaminated with PHCs. Accordingly, this experimental research aimed to estimate the potential of thermal water vapor and air plasmas to de-pollute soil contaminated with often-used PHCs – diesel. Also, the effect of the contaminant content in the soil during the de-pollution process was investigated. Thus, in this study, the feasibility of the thermal plasma remediation method was confirmed by experimental research and the analysis of the soil properties and generated remediation reaction products applying state-of-the-art analysis methods, including scanning electron microscopy, energy-dispersive X-ray spectroscopy, elemental analyzer (CHNS analysis), thermogravimetric analysis and differential scanning calorimetry, and multi-component gas analyzer. The performed experimental research revealed that 99.9% of PHCs – diesel contaminant removal efficiency can be achieved by performing contaminated soil de-pollution process in the environment of the thermal plasma in defiance of whether water vapor or air was used as a plasma-forming gas. Furthermore, it was found that the soil's contaminant content (80–160 g/kg) did not influence its' removal efficiency. Finally, it was established that PHCs – diesel was decomposed into producer gas mainly consisting of H_2, CO (also called synthesis gas) and CO_2. Consequently, the thermal plasma provides a way not only to de-pollute the soil rich with contaminants but also to use the PHCs present in the soil again by breaking it down into gaseous products that can further be used to meet human consumerism needs.

The application of the *ex-situ* thermal plasma remediation method focuses on the highly PHCs-polluted soil found in industrial areas, oil product storage areas (e.g., former oil bases), or other polluted areas (e.g., in the area of forest land) where contaminated soil must be collected and replaced with clean soil. Meanwhile, contaminated soil is being taken away to remediate it by applying *ex-situ* remediation methods.

2. Methodology

2.1. Material used

The clean and humus-rich soil was gathered from one of the Lithuania regions – Kaunas. First, the soil was dried for 24 h in the furnace at 70 °C and then sifted from debris and stones using 2 mm mesh to guarantee fluent soil feeding into the plasma-chemical reactor. Sieved humus-rich soil was synthetically contaminated with three distinct diesel concentrations (80 g/kg, 120 g/kg, and 160 g/kg). Such pollutant concentrations were chosen based on the diesel content found under real conditions in Lithuania's soil.

2.2. The soil's ultimate and proximate analysis

The ultimate and proximate analysis of the clean humus-rich and diesel-contaminated soil was performed before the soil remediation process in the plasma environment and is presented in Table 1. Ultimate analysis specified that soil contamination with diesel enhanced carbon concentration from 10.92 wt% in the clean soil to 11.28–16.52 wt% in the soil contaminated with 80–160 g/kg of diesel. A similar trend was found with hydrogen and nitrogen concentrations, which increased to 1.17–1.78 wt% and 0.30–0.35 wt%, from the initial concentrations of 0.96 wt% and 0.18 wt%, respectively, of the clean humus-rich soil. Also, the same 0.05 wt% concentration of sulfur persisted in the soil.

Proximate analysis showed that ash content in the soil decreased from primary 85.56 wt% in the clean soil to 79.01–72.58 wt%, with the enhancement of contaminants concentrations in the soil. Also, the moisture content in the soil increased from 1.32 wt% in the clean soil to 1.60–2.25 wt% in the soil contaminated with 80–160 g/kg of diesel.

2.3. Remediation system of contaminated soil

The experimental research parameters of the diesel-contaminated soil remediation in the plasma environment are shown in Table 2. The remediation process was carried out at a plasma torch power of 52.8–56 kW, water vapor flow rate of 5.14 g/s, airflow rate of 4.97 g/s and contaminated soil flow rate of 1.5 g/s. The contaminated soil remediation process was conducted under atmospheric pressure for almost half an hour (27 min). Thus, in each experiment (80–160 g/kg of diesel in the soil), about 2.4 kg of PHCs-diesel contaminated soil was de-polluted. Accordingly, the presented *ex-situ* plasma-based soil remediation system has the capacity to de-pollute about 5.4 kg/h of contaminated soil.

Table 1
The ultimate and proximate analysis of the clean and diesel-contaminated soil.

Ultimate analysis	Clean humus-rich soil, wt %	Humus-rich soil contaminated with diesel, wt %		
		80 g/kg[1]	120 g/kg	160 g/kg
Carbon (C)	10.92 ±2.05	11.28 ±2.97	14.40 ±2.51	16.52 ±2.63
Hydrogen (H)	0.96 ± 0.43	1.17 ± 0.43	1.64 ± 0.42	1.78 ± 0.44
Nitrogen (N)	0.18 ± 0.30	0.31 ± 0.31	0.30 ± 0.31	0.35 ± 0.31
Sulfur (S)	0.05 ± 0.29	0.05 ± 0.27	0.05 ± 0.28	0.05 ± 0.28
Oxygen (O)[2]	1.01	6.58	7.25	6.94
Proximate analysis				
Moisture	1.32 ± 0.05	1.60 ± 0.06	2.25 ±0.09	1.78 ± 0.07
Ash	85.56 ± 3.42	79.01 ± 3.16	74.11 ± 2.96	72.58 ± 2.90

1 Diesel concentration in the soil, g/kg.
2 By difference.

Table 2
The experimental parameters of the diesel-contaminated soil remediation process in the plasma environment.

Diesel-contaminated soil remediation using:		
Parameter	Air plasma	Water vapor plasma
Arc current, A	160	160
Arc voltage, V	330	350
Power, kW	52.8	56
Soil feed rate, g/s	1.5	1.5
Gasifying agent flow rate, g/s	4.97	5.14
Diesel amount in the soil, g/kg	80, 120, 160	80, 120, 160
Mean T_{plasma}, K	4100	2800
Plasma torch thermal efficiency (η), %	60–73	78–79

The mean operating temperature of the water vapor plasma and air plasma systems were equal to 2800 K and 4100 K, respectively.

The plasma-based soil remediation system is presented in Fig. 1. The system is composed of a soil feeder (1), a DC arc plasma torch (2), a plasma-chemical reactor (the dimension: 1 m long and 0.4 m in diameter) (3), a power supply system – rectifier DC (4), an air supply system (5), a steam generator (6), a superheater (7), a water filter for particulate matter (8), a condenser (9), and a gas analyzer equipped with a producer gas analysis system (10).

The feedstock feeder is installed at the top of the plasma-chemical reactor so that the soil grains can drop straight to the bottom of the reactor. The DC arc plasma torch also is fitted at the upper part of the plasma-chemical reactor and is oriented at 45° angle to the soil flow. Such construction provides sufficient conditions for interacting soil contaminants with active species in the plasma environment, thus ensuring the remediation process.

2.4. Equipment used for the analysis of soil and producer gas

Soil analysis was carried out before and after the remediation process in the thermal water vapor or air plasma environments. Scanning electron microscopy (SEM, Hitachi S–3400N) characterized the soil surface morphology. The energy-dispersive X-ray spectroscopy (EDX, Bruker Quad 0540) was applied to identify clean, contaminated, and plasma-remediated soil elemental composition. The FLASH 2000 elemental analyzer was used to evaluate the soil's ultimate analysis (CHNS). The clean and diesel-contaminated soil's carbon, hydrogen, and nitrogen measurements were carried out according to LST EN ISO 16948:2015 standard requirements. The sulfur content was evaluated according to the BM-8B/3-BO0:2012 methodical. The oxygen content was calculated by the difference. Thermal properties of pure diesel, clean and diesel-contaminated soil were estimated by the thermogravimetric analysis (TGA/DTG) and differential scanning calorimetry (DSC)) using NETZSCH STA 449 F3 Jupiter analyzer with a SiC furnace. The quantification of produced gas concentrations, which were generated via the remediation process of diesel-contaminated soil in the thermal plasma's environment, was done by the multi-component gas analyzer (MRU SWG 300^{-1}). The above-presented research equipment was applied for the soil analysis three times to guarantee data reliability. The data presented in this experimental research paper are the mean value of these replicates. The measurements' relative error with EDX, TGA, and gas analyzer is ±1–2%, ±4% and ±2%, respectively.

2.5. Basic reactions taking place in a plasma-based soil remediation system

The ability to carry out diesel-contaminated soil remediation in the plasma-chemical reactor begins with the formation of the plasma environment. Plasma is described as a partially or fully ionized gas. The plasma stream comprises electrons, positive and negative ions, and neutral species, including various atoms, molecules, radicals, and excited species. At least part of the plasma species is in electronically excited states, which creates a highly reactive environment needed for the chemical reactions (Gimžauskaitė et al., 2022; Wang et al., 2018; Zheng et al., 2010).

The formation of the reactive radicals appears during the interaction between the energetic electrons emitted from the cathode and the gases (Fig. 1). The type of reactive radicals depends on the kind of plasma forming gas. In the case of water vapor serving as a plasma-forming gas, the plasma reactive species, including O•, H• and OH•, are formed via the chemical reactions which are given beneath (Judée et al., 2018; Kapaldo et al., 2019; Wang et al., 2018):

$$H_2O + e^- \rightarrow H\bullet + OH\bullet + e^- \quad (1)$$

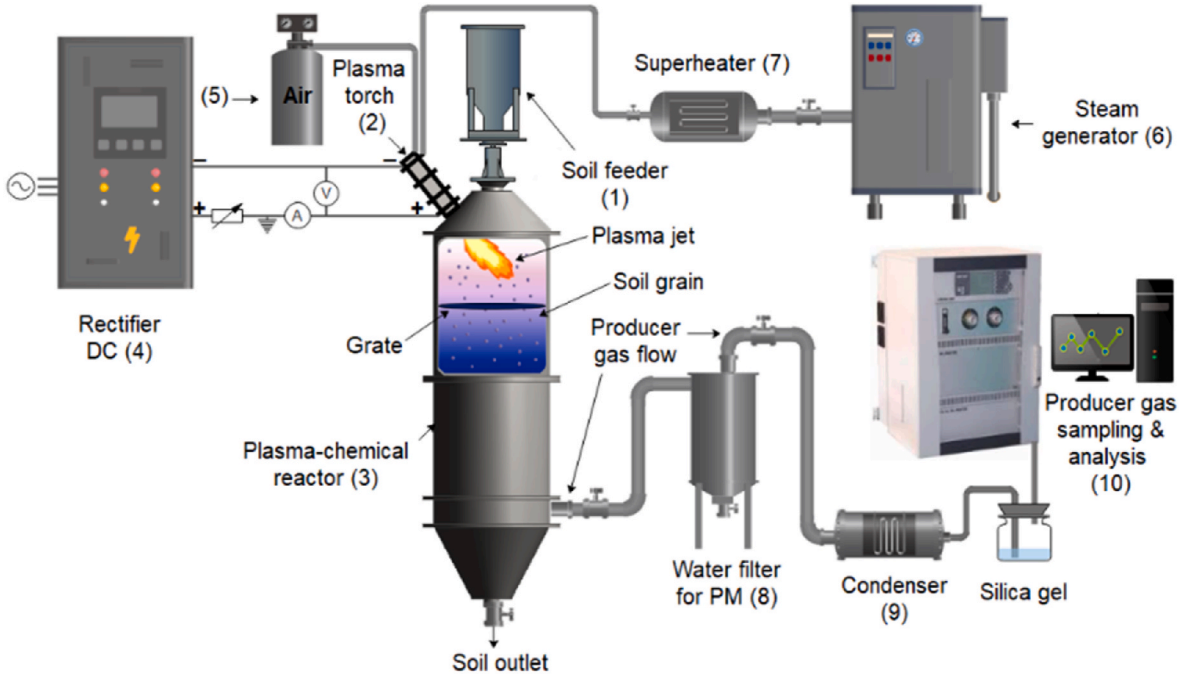

Fig. 1. The *ex-situ* plasma-based soil remediation system.

$$H_2O + O\bullet \rightarrow 2OH\bullet \quad (2)$$

$$H_2 + O\bullet \rightarrow OH\bullet + H\bullet \quad (3)$$

$$H_2 + OH\bullet \rightarrow H_2O + H\bullet \quad (4)$$

When air is applied as a plasma-forming gas, the plasma reactive species (O•, N•) are generated via the chemical reactions shown beneath (Equations (5) and (6)). Also, the produced plasma reactive species can participate in the gas-phase reactions during which nitrogen oxides can be formed (Equations (7) and (8)) (Sanito et al., 2022; Shen et al., 2019; Topolovec et al., 2022).

$$O_2 + e^- \rightarrow 2O\bullet + e^- \quad (5)$$

$$N_2 + e^- \rightarrow 2N\bullet + e^- \quad (6)$$

$$N\bullet + O\bullet \rightarrow NO \quad (7)$$

$$NO + O\bullet \rightarrow NO_2 \quad (8)$$

The diesel conversion general chemical reactions (9–14) are presented below (Lee et al., 2010; Martin et al., 2015; Peters et al., 2018; Piqueras et al., 2019; Song et al., 2020):

Steam reforming:

$$C_nH_m + nH_2O \leftrightarrow nCO + \left(\frac{m}{2} + n\right) H_2 \quad (9)$$

Water-gas shift reaction:

$$CO + H_2O \leftrightarrow CO_2 + H_2 \quad (10)$$

Partial oxidation:

$$C_nH_m + \frac{n}{2}O_2 \rightarrow nCO + \frac{m}{2}H_2 \quad (11)$$

$$C_nH_m + \frac{n}{2}(O_2 + 3.76N_2) \rightarrow nCO + \frac{m}{2}H_2 + 1.88nN_2 \quad (12)$$

$$C_nH_m + n(O_2 + 3.76N_2) \rightarrow nCO_2 + \frac{m}{2}H_2 + 3.76nN_2 \quad (13)$$

Complete oxidation:

$$C_nH_m + \left(n + \frac{m}{4}\right)O_2 \rightarrow nCO_2 + \frac{m}{2}H_2O \quad (14)$$

In addition to the general reactions (Eqs. (9)–(14)), the side reactions (Eq. (15)–(17)), such as the formation of the coke, can also appear:

Boudouard reaction:

$$2\,CO \leftrightarrow CO_2 + C \quad (15)$$

Reverse gasification:

$$CO + H_2 \leftrightarrow C + H_2O \quad (16)$$

Decomposition:

$$C_nH_m \leftrightarrow nC + m/2H_2 \quad (17)$$

The given reactions will aid in explaining and comprehending the experimental results obtained during the diesel-contaminated soil remediation process, which are presented in the following section.

Moreover, visualizing the basic mechanism of the PHCs de-pollution in the plasma environment is also useful. Accordingly, when the soil faces the pollution process, the PHCs cover soil grains and first form the upper layer above it. Secondly, the PHCs penetrate the soil's inner layers and are absorbed within the pores. The higher the PHCs concentration, the more the soil is compressed and flattened, reducing soil porosity. Also, the increasing pollutant concentration forms a thicker upper layer above soil grains.

Furthermore, the PHCs contaminated soil de-pollution process in the thermal plasma environment comprises several chemical reactions (Eqs. (1)–(17)), which was presented above. The process starts with the formation of the thermal plasma environment. The plasma torches cathode emits energetic electrons, which interact with plasma-forming gas (air or water vapor), forming the reactive plasma species (Eqs. (1)–(8)). Consequently, a rich in reactive species plasma environment warrants efficient PHCs decomposition reactions (Eqs. (9)–(17)), which vary depending on the type of plasma forming gas. Firstly, the de-pollution process appears at the top layer of the soil. At this level, reactive plasma species interact with the upper layer of PHCs located above soil grains and decompose it. Further, when the upper pollutant layer is handled, active plasma species penetrate the soil pores and react with PHCs in inner soil layers. Thus, the soil de-pollution process in the plasma environment occurs gradually in the vertical direction of the soil layers. The interaction between PHCs and the reactive plasma species leads to the PHCs splitting into producer gas (mostly formed of H_2, CO, and CO_2).

3. Results and discussion

3.1. Examination of the soil surface morphology

The surface morphology images of clean soil, soil contaminated with 80–120 g/kg of PHCs–diesel, and remediated soil in the ambient of water vapor plasma or air plasma is provided in Fig. 2. The granular structure was visible in all soil samples regardless of whether the soil was clean, contaminated or remediated. Further, the roughness of the PHCs–diesel contaminated soil surface growth compared to the clean soil (Fig. 2 b, c, d). Also, the merge of the soil grains and the more significant agglomeration formation was seen in the image of soil contaminated with the highest (160 g/kg) PHCs–diesel concentration (Fig. 2 d). The properties of the humus-rich soil possibly influence such a tendency. This type of soil easily crumbles compared to the loamy–sandy soil analyzed in our previous study (Gimžauskaitė et al., 2020). Therefore, only a higher concentration of PHCs–diesel caused the soil particles to stick together into larger clods. Meanwhile, in the case of the loamy-sandy soil, the soil grains' stickiness effect was apparent in all contaminated soil samples with a diesel concentration of 80–160 g/kg.

Moreover, after the PHCs–diesel contaminated soil de-pollution process in the water vapor plasma or air plasma environments, the soil surface demonstrated relatively smoothness close to clean soil.

3.2. Soil elemental composition analysis

The elemental composition of the soil before and after the de-pollution process in the environment of the water vapor plasma or air plasma is given in Table 3. The alteration of the concentration of the carbon component in the soil was noticed when the soil was contaminated with PHCs–diesel and when it was de-polluted using water vapor plasma or air plasma. More precisely, the carbon concentration in the clean soil was equal to 9.8 wt%. Still, after the soil contamination with PHCs–diesel, the carbon concentration increased to 11.3 wt%, 12.7 wt% and 14.2 wt% when contaminant content in the soil was equal to 80 g/kg, 120 g/kg and 160 g/kg, respectively.

Further, the soil de-pollution process in the plasma environment influenced the decrease of the carbon concentration in the soil regardless of the gas type (water vapor or air) used to form the plasma. In both cases, the carbon content in the soil reduced to 3–6 wt%. Such carbon reduction tendency shows that PHCs–diesel (average formula: $C_{12}H_{23}$) was decomposed from the soil, and the soil de-pollution process succeeded. However, the plasma-based remediation method also affected the natural carbon reserves in the soil since the carbon content after the remediation process was lower (3–6 wt%) compared to the primary carbon content (9.8 wt%) in the clean soil. Thus, part of the natural carbon was evaporated during the soil de-pollution process. Moreover, the sulfur content in the soil was not recorded after the soil de-pollution process. Possibly, as a component of clean soil and diesel, the sulfur was

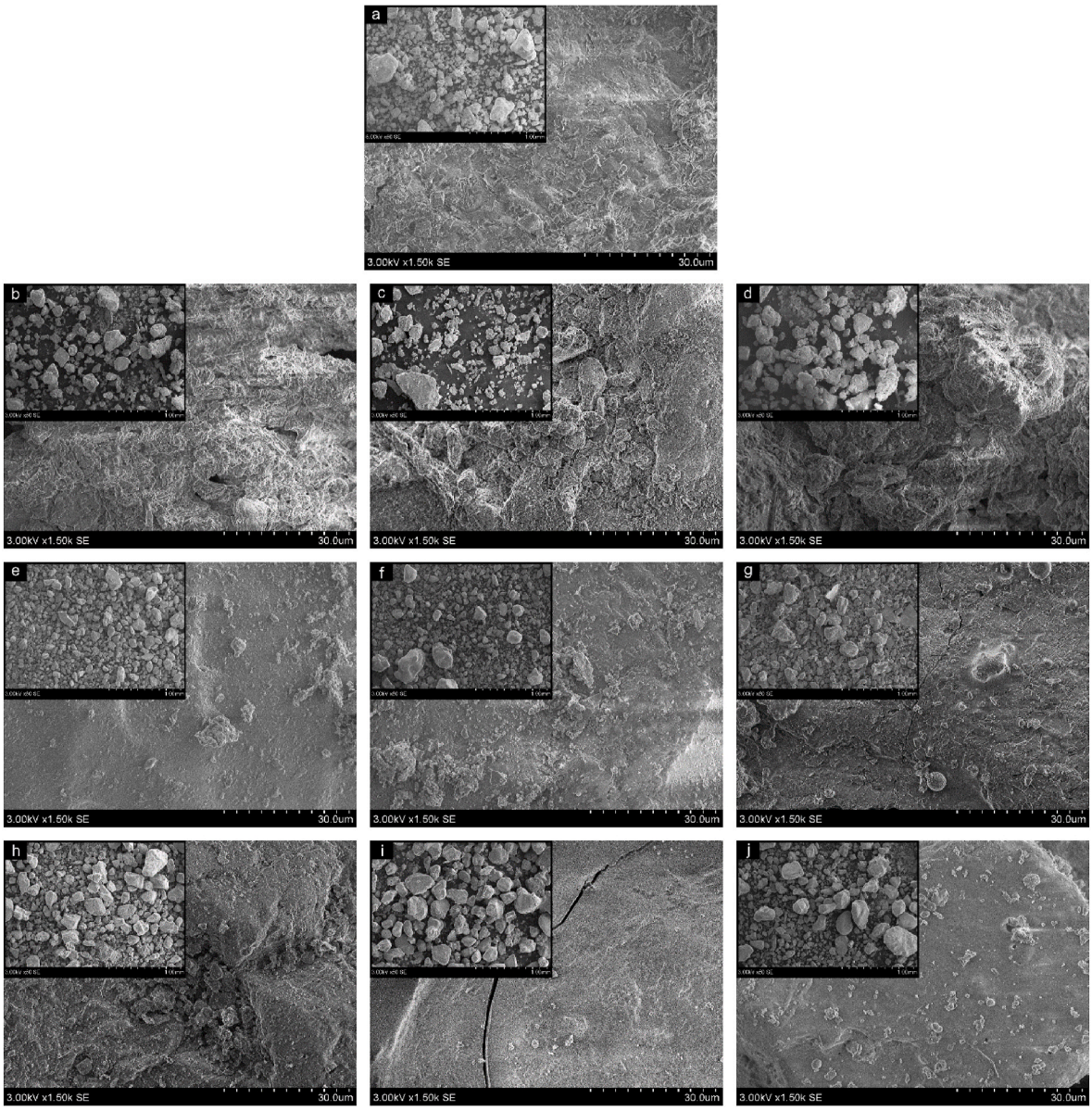

Fig. 2. The SEM images of soil surface: a – clean soil; b, c, d – soil contaminated with PHCs–diesel 80 g/kg, 120 g/kg, and 160 g/kg, respectively; e, f, g – de-polluted soil in the water vapor plasma environment; h, i, j – de-polluted soil in the air plasma environment.

volatilized during soil remediation. Furthermore, since minerals in the soil do not participate in the volatilization process but instead remain unchanged or recrystallize into secondary minerals (Snellings et al., 2012), their concentrations after the soil de-pollution process using the plasma altered negligibly.

3.3. Thermal analysis of the soil

Seeking to determine PHCs–diesel conduct in the humus-rich soil within the de-pollution process, the TGA (TG), DTG and DSC evaluations were carried out during the combustion process (Fig. 3 a-e). In the first place, the measurement was performed with clean humus-rich soil (Fig. 3 a).

The pure soil's combustion process consisted of the three mass loss stages (TG, DTG curves). The first one corresponded to the soil's moisture content reduction (1.32% recorded from 0 to 14.5 min). Under TGA and DTG data, the second mass loss of the sample appeared in the range of 14.5–24.5 min of the measurement, and it reflected the reduction of the organic matter and volatiles (8.27%) in the analyzed soil. Finally, the third mass loss stage (between 24.5 and 33 min) represented the reduction of the soil's remaining organic part (4.86%). During the combustion process, 85.56% of the ash was generated.

Further, the pure PHCs–diesel thermal analysis was performed (Fig. 3 b). The combustion process of pure diesel consisted of one mass loss stage (35.72%) and DTG negative peak (at 243.8 °C), which appeared from 0 to 16.5 min. This measurement revealed the exact time and temperature of the pure diesel combustion. It was necessary to understand better the further thermal analysis with PHCs–diesel contaminated soil.

Finally, research was performed with the soil polluted by 80 g/kg, 120 g/kg and 160 g/kg of PHCs–diesel (Fig. 3 c-e). Four stages of mass loss were recorded despite the contaminant content in the soil. The first mass loss stage showed a decrease in the soil moisture amount (1.6–2.25%), while the first DTG negative peak (the second mass loss stage) measured in the range of 10–16 min (at 197.1–254.6 °C) identified the volatile organic compounds (VOCs) vaporization and combustion. The obtained tendency coincides with the trend obtained during the thermal analysis of pure diesel (Fig. 3 b). Thus, it could be stated that

Table 3
The elemental composition of the clean, PHCs–diesel contaminated and de-polluted soil.

Element	Clean soil, wt[a]%	Soil contaminated with diesel, wt %		
		80 g/kg[b]	120 g/kg	160 g/kg
Carbon	9.86	11.30	12.73	14.19
Oxygen	49.40	49.63	49.54	49.12
Silicon	20.77	21.56	22.28	21.21
Potassium	1.88	1.79	1.27	1.24
Calcium	10.20	8.46	7.68	7.63
Magnesium	1.14	0.83	0.79	0.74
Aluminum	3.37	3.28	2.73	2.93
Iron	2.31	2.16	2.04	1.79
Sodium	0.19	0.23	0.21	0.31
Titanium	0.52	0.49	0.46	0.56
Sulfur	0.37	0.29	0.29	0.28

Element	Soil remediated with water vapor plasma, wt %			Soil remediated with air plasma, wt %		
	80 g/kg	120 g/kg	160 g/kg	80 g/kg	120 g/kg	160 g/kg
Carbon	4.17	3.22	5.93	4.76	3.11	5.71
Oxygen	46.15	47.40	45.56	51.46	50.86	50.12
Silicon	29.61	29.47	27.82	27.75	29.45	28.73
Potassium	2.22	1.82	2.10	1.51	1.86	1.81
Calcium	9.94	10.39	11.25	7.62	7.68	7.21
Magnesium	0.96	1.10	1.11	0.84	0.94	0.86
Aluminium	3.99	3.50	3.18	3.41	2.99	3.05
Iron	2.10	2.25	2.27	1.96	2.16	1.86
Sodium	0.41	0.41	0.39	0.19	0.39	0.23
Titanium	0.46	0.45	0.40	0.50	0.56	0.42
Sulfur	n.d.	n.d.	n.d.	n.d.	n.d.	n.d.

[a] Weight concentration of element, wt %.
[b] Diesel concentration in the soil, g/kg.

the second mass loss stage of the contaminated soil thermal analysis reveals the decomposition of diesel from the soil. Meanwhile, the reduction of the volatiles and char content in the soil is reflected by the third and four stages of the mass loss in the same way as in the case of the thermal analysis of the clean soil. Also, the generation of the ash was recorded during the thermal analysis of the diesel-polluted soil (79.01–72.58%). Furthermore, the curves of the DSC indicate the endothermic process.

3.4. Generated gaseous products analysis

3.4.1. Gaseous products composition after soil remediation in the water vapor plasma environment

The highest and average values of producer gas concentrations generated during the soil de-pollution process with water vapor plasma are provided in Table 4. The synthesis gas (H_2+CO) and CO_2 concentrations grew with the increase of the PHCs–diesel content in the soil from 80 g/kg to 120 g/kg, respectively. Meanwhile, the H_2, CO and CO_2 concentrations reduced when the soil was polluted with 160 g/kg of the PHCs–diesel. The content of NO, NO_2, SO_2 and C_3H_8 varied negligibly in all three experimental cases.

The changes in the producer gas concentrations measured via the soil de-pollution process in the water vapor plasma environment are given in Fig. 4.

While oxygen content decreased from 21 vol% to 1.74–0.34 vol%, carbon-based materials (PHCs–diesel) were mainly transformed into gaseous compounds, including synthesis gas (H_2+CO) and CO_2 in all three experimental cases. Therefore, up to 25.33–37.50 vol% of hydrogen and up to 5.27–9.25 vol% of CO were recorded during the soil de-pollution process. Also, 16.52–19.43 vol% of carbon dioxide was generated. The formation of the synthesis gas was influenced due to the predominant steam reforming (Eq. (9)) and decomposition (Eq. (17)) reactions. The appearance of the CO_2 was noticed due to the prevailing water-gas shift (Eq. (10)) and Boudouard (Eq. (15)) reactions.

The highest synthesis gas amount was generated during the de-pollution process of the soil contaminated with 120 g/kg of PHCs–diesel. Such tendency was mainly affected by two factors: the higher contaminant content in the soil compared to 80 g/kg of PHCs–diesel and the prevailing fast steam reforming reaction (Eq. (9)). Nevertheless, in the case when the soil was polluted with the highest PHCS – diesel concentration (160 g/kg), the steam reforming reaction slowed down causing the increase of the time needed for the active plasma species to react with contaminant molecules. Also, the higher contaminant content meant that the competition for active plasma species appeared between contaminant molecules. Furthermore, the higher pollutant content formed the thicker covering layer above the soil grains. Consequently, active plasma species required more time and energy first to decompose the PHCs–diesel molecules deployed at the topsoil layer and, finally, decompose contaminant molecules located in the inner layers of the soil. Hence, the soil de-pollution process slowed down, and it caused the generation of the lower content of the synthesis gas. The same trend was observed studying the loamy-sandy soil remediation process in the water vapor plasma environment (Gimžauskaitė et al., 2020). Furthermore, the reverse gasification reaction (Eq. (16)) could also have influenced the formation of a lower content of synthesis gas.

Moreover, small concentrations of the NO (0.51–0.56 vol%), NO_2 (0.05–0.07 vol%), SO_2 (0.05–0.07 vol%), and C_3H_8 (0.16–0.27 vol%) were recorded in all three cases (Fig. 4 b, d, f). Such tendency of the formation of the gaseous compounds was caused by reactions between the active plasma species and the PHCs–diesel. Also, a small amount of air (~13%) was used to protect the plasma torches' cathode from erosion. Thus, air also contributed to the formation of these gaseous compounds.

3.4.2. Gaseous products composition after soil remediation in the air plasma environment

The highest and average values of producer gas concentrations obtained during the soil remediation with air plasma are shown in Table 5. The obtained results showed that CO_2 was the main produced gaseous product, followed by the traces of the synthesis gas. The highest values of the CO_2 concentration increased with the increase of the PHCs–diesel content in the soil from 80 g/kg to 120 g/kg. However, CO_2 content decreased with further growth of the soil's pollutant concentration (160 g/kg). The concentrations of NO, NO_2, SO_2 and C_3H_8 changed insignificantly in all three experimental cases.

The changes in the producer gas concentrations during the interaction between the PHCs–diesel polluted soil and air plasma are given in Fig. 5.

Formation of the CO_2 was observed during the de-pollution process of the soil polluted with 80 g/kg and 120 g/kg of PHCs–diesel, respectively. Thus, the highest measured CO_2 concentrations corresponded to 12.17 vol% and 13.17 vol% when the content of PHCs–diesel in the soil were equal to 80 g/kg and 120 g/kg, respectively (Fig. 5 a, c). Meanwhile, the oxygen content decreased to 4.93 vol% and 1.96% from its initial 21 vol% concentration when the de-pollution of the soil contaminated with 80 g/kg and 120 g/kg of PHCs–diesel took place. This tendency was observed due to the predominant PHCs–diesel complete oxidation reaction (Eq. (14)).

Moreover, when the PHCs–diesel content in the soil was increased to 160 g/kg, the generation of the CO_2 (up to 12.63 vol%), H_2 (up to 1.67 vol%) and CO (up to 4.66 vol%) was measured (Fig. 5 e). Consequently, during the soil de-pollution process, the complete oxidation reaction (Eq. (14)) took place, and the formation of the CO_2 was observed. But the environment with the lack of oxygen was formed after a while. Such changes in the ambient conditions slowed down the complete oxidation reaction (Eq. (14)) and induced the partial oxidation reactions (Eq. (11)–(13)) prevailing. Consequently, the H_2 and CO (synthesis gas) generation was recorded.

Further, low concentrations of the NO (0.13–0.2 vol%), NO_2

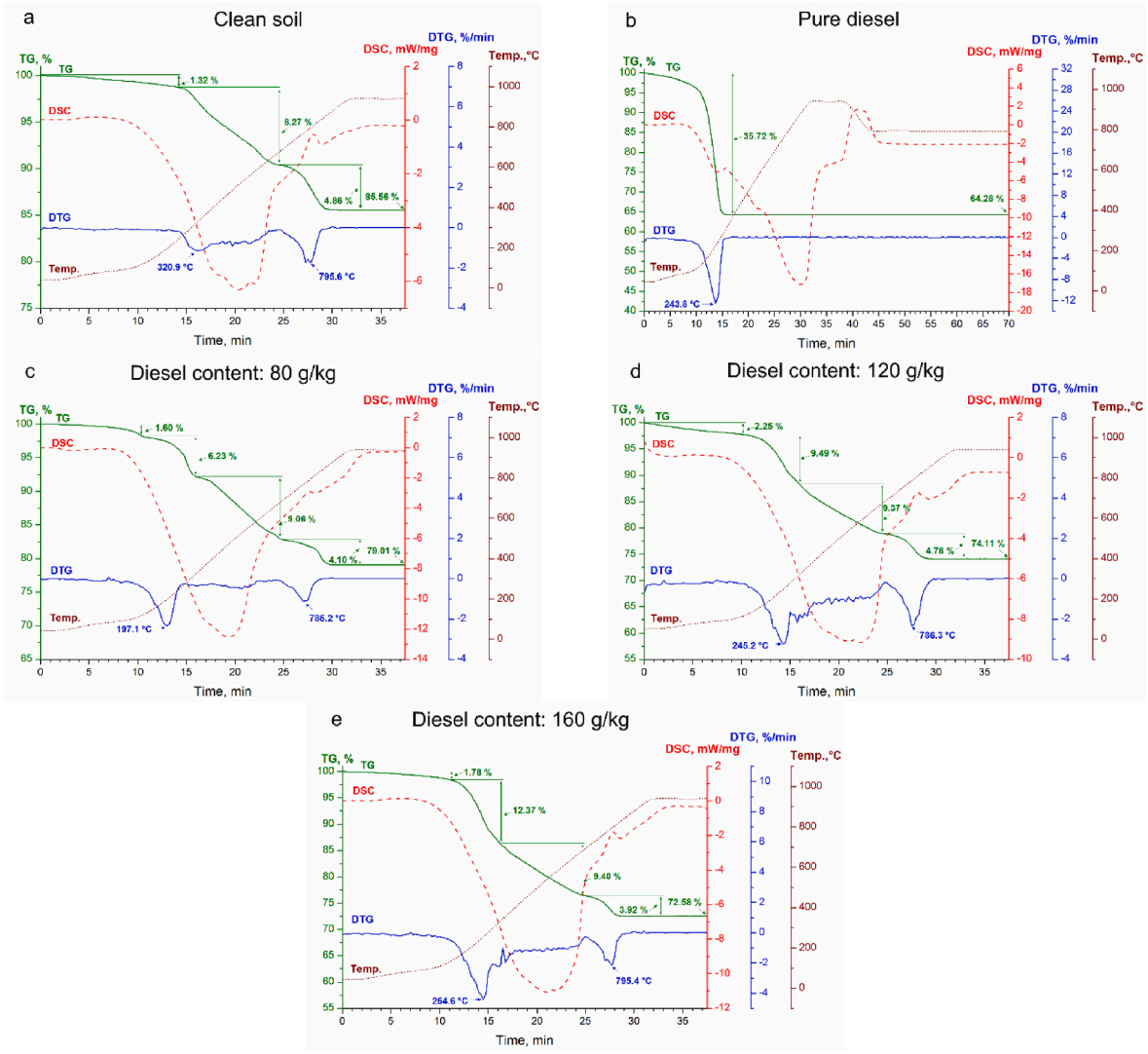

Fig. 3. Mass loss dynamics during the process of the combustion: a – clean soil; b – pure diesel; c, d, e – soil polluted with 80 g/kg, 120 g/kg, and 160 g/kg of PHCs–diesel, respectively.

Table 4
Producer gas concentrations obtained during the soil remediation process.

Diesel concentration:	Gas concentrations extracted during the soil remediation with water vapor plasma:					
	80 ± 3 g/kg		120 ± 3 g/kg		160 ± 3 g/kg	
	Highest value, %	Average value, %	Highest value, %	Average value, %	Highest value, %	Average value, %
H_2	37.50	27.20	41.90	23.89	25.33	16.73
CO	9.17	6.75	9.25	5.55	5.27	3.70
CO_2	16.52	11.69	19.43	12.65	18.31	13.24
NO	0.51	0.34	0.56	0.38	0.55	0.38
NO_2	0.05	0.03	0.06	0.04	0.07	0.05
SO_2	0.07	0.05	0.06	0.04	0.05	0.04
C_3H_8	0.27	0.19	0.20	0.15	0.16	0.12

(0.04–0.05 vol%), SO_2 (0.001–0.014 vol%), and C_3H_8 (0.001–0.044 vol %) were measure in all three experimental cases (Fig. 5 b, d, f). Similarly, as in the case of using the water vapor plasma, the generation of NO, NO_2, SO_2, and C_3H_8 was mainly related to the PHCs–diesel composition and the use of air to form the plasma environment.

3.5. The potential to remediate soil contaminated with petroleum compounds by applying plasma technologies

The experiment's objective was remediating soil from the PHCs–diesel. Accordingly, the thermal plasma potential to remediate soil contaminated with the PHCs–diesel is provided in Table 6. After the de-pollution process, soil samples were analyzed under the normative document LAND-89-2010. The PHCs–diesel concentration in the soil samples was not found or was below the laboratory detection limit

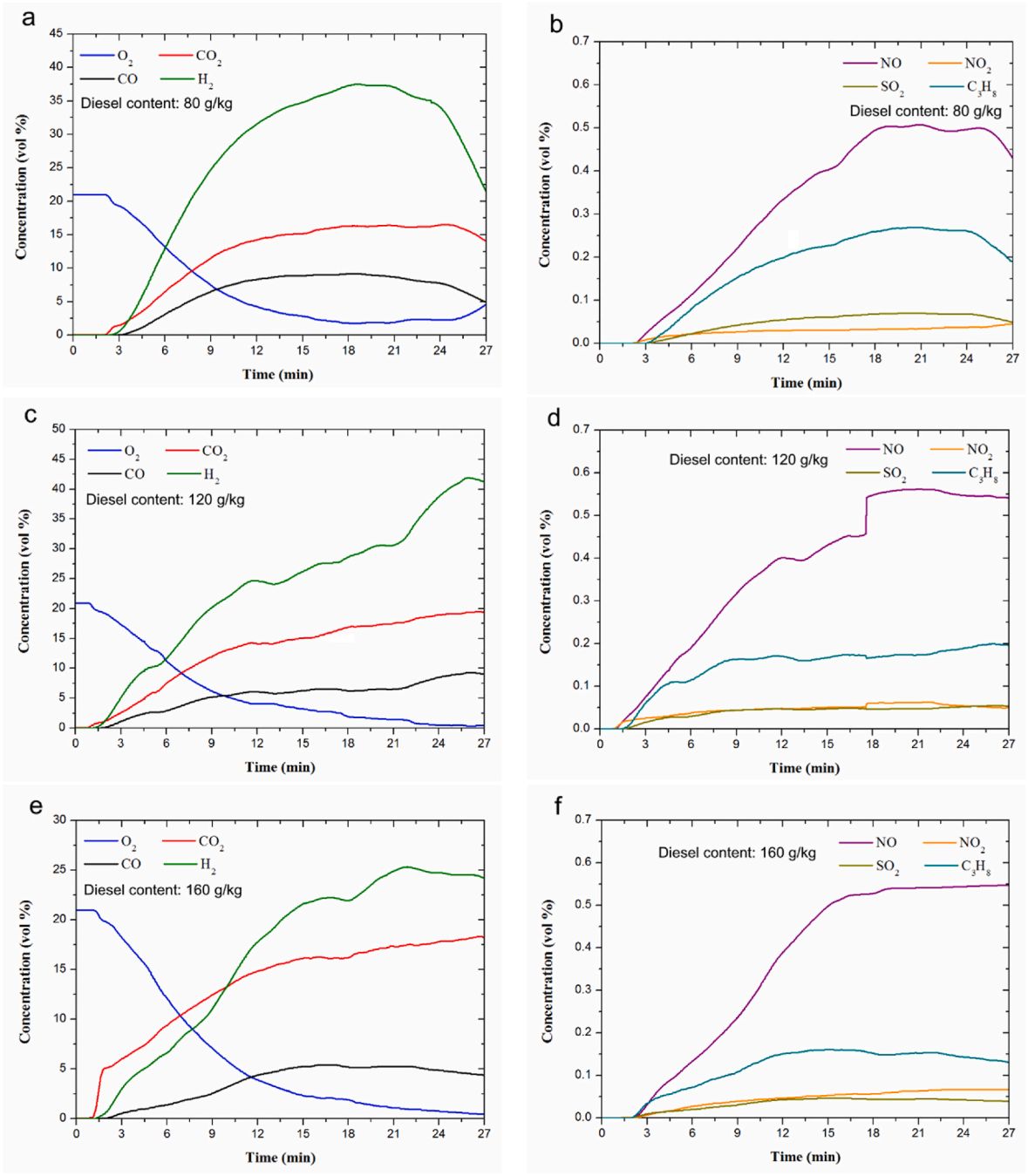

Fig. 4. Concentrations of producer gas measured during the soil de-pollution process: a-f – soil polluted with 80 g/kg, 120 g/kg, and 160 g/kg of PHCs–diesel, respectively. The soil de-pollution process was performed with water vapor plasma.

Table 5
Producer gas concentrations obtained during the soil remediation process.

Diesel concentration:	Gas concentrations extracted during the soil remediation with air plasma:					
	80 ± 3 g/kg		120 ± 3 g/kg		160 ± 3 g/kg	
	Highest value, %	Average value, %	Highest value, %	Average value, %	Highest value, %	Average value, %
H_2	0.12	0.01	0.25	0.08	1.65	0.64
CO	0.1	0.02	1.16	0.40	4.64	2.01
CO_2	12.16	6.32	13.13	6.72	12.61	9.09
NO	0.21	0.10	0.35	0.15	0.27	0.14
NO_2	0.05	0.03	0.05	0.03	0.04	0.03
SO_2	0.001		0.002		0.001	
C_3H_8	0.001		0.011	0.005	0.003	0.002

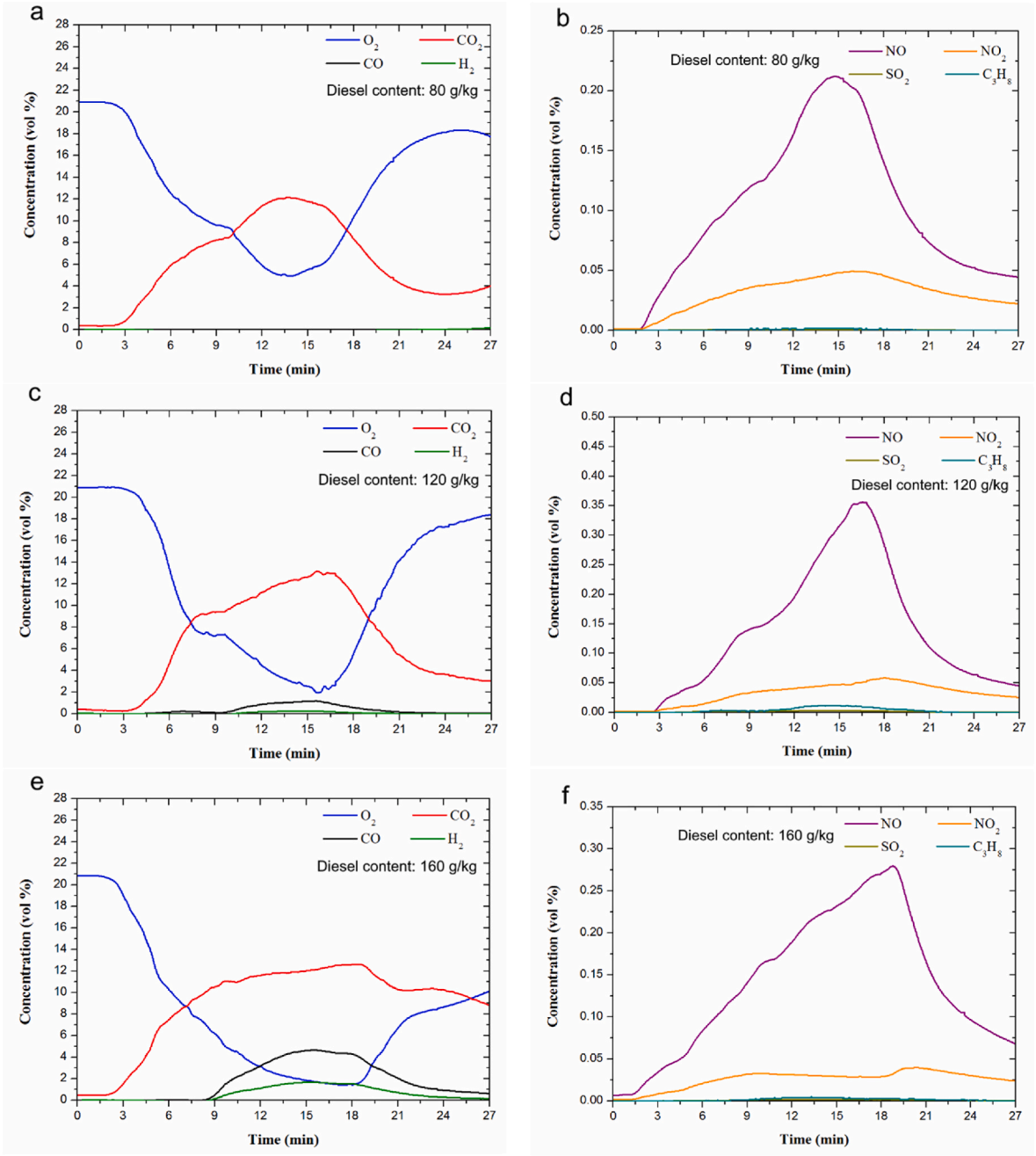

Fig. 5. Concentrations of producer gas measured during the soil de-pollution process: a-f – soil polluted with 80 g/kg, 120 g/kg, and 160 g/kg of PHCs–diesel, respectively. The soil de-pollution process was performed with air plasma.

Table 6
The thermal plasma potential to remediate soil contaminated with diesel (80 g/kg, 120 g/kg and 160 g/kg).

Parameter	Water vapor plasma	Air plasma
PHCs–diesel content in the soil after remediation	<0.089 g/kg	<0.089 g/kg
Contaminant removal efficiency, %	99.9	99.9

(<0.089 g/kg). Consequently, experimental results showed that both types of plasma (water vapor and air) are appropriate to de-pollute soil contaminated with PHCs–diesel. Additionally, the environment of the thermal plasma provides high contaminant removal efficiency.

Also, a brief comparison of the remediation of soil contaminated with petroleum products by applying different plasma technologies is presented in Table 7. Correspondingly, the contaminated soil remediation with thermal plasma assured 99.9% contaminant removal efficiency of relatively high contents of PHCs–diesel (80 g/kg, 120 g/kg and 160 g/kg) from the soil in a short time (27 min). Meanwhile, the pollutant removal efficiency from the soil applying non-thermal plasma ranged between 23.0 and 98.5%.

Seeking to give a little more insight into non-thermal plasma application for soil de-pollution, a few key research findings from several researchers working in the field are provided below.

Zhao et al. (2021) applied dielectric barrier discharge (DBD) plasma for diesel fuel degradation from the soil. While evaluating the influence of the initial diesel fuel concentration in the soil, researchers noted that 62% contaminant removal efficiency was reached after 40 min of

Table 7
Comparison of petroleum products contaminated soil remediation by various plasma methods.

Reference	Discharge type, power kW	Gasifying agent	Soil pollutant	Pollutant content, g/kg	Treatment time, min	Removal efficiency, %
This work	DC, 56.00	Water vapor	Diesel fuel	80–160	27	99.9
This work	DC, 52.80	Air	Diesel fuel	80–160	27	99.9
Zhao et al. (2021)	DBD, 0.18	–	Diesel fuel	5–10	40	62.0–74.0
Wong et al. (2022)	TPB + H_2O_2[1], 10–20 kV	–	Diesel fuel	2	180	88.90–98.50
Zhan et al. (2019)	PCD, 0.02–0.06	Air	Gasoline	2–4	60	86.0
Zhan et al. (2019)	PCD, 0.02–0.06	O_2	Gasoline	2–4	60	84.0
Zhan et al. (2019)	PCD, 0.02–0.06	Ar	Gasoline	2–4	60	39.0
Zhan et al. (2019)	PCD, 0.02–0.06	N_2	Gasoline	2–4	60	23.0
Li et al. (2017)	PCD, 30 kV	–	Gasoline	2.5–10	60	57.0–81.0
Zhao et al. (2023)	DBD, 0.081	–	Gasoline	2–8	60	72.0–91.0
Zhao et al. (2023)	DBD, 0.081	Air	Gasoline	5	60	92.0
Zhao et al. (2023)	DBD, 0.081	O_2	Gasoline	5	60	87.0
Zhao et al. (2023)	DBD, 0.081	Ar	Gasoline	5	60	~100
Zhao et al. (2023)	DBD, 0.081	N_2	Gasoline	5	60	59.0
Aggelopoulos (2016)	DBD, 0.025	Air	n-dodecane	0.5–50	22	84.0–94.0
Aggelopoulos (2016)	DBD, 0.025	Air	n-dodecane	0.5–50	34	91.0–97.0
Redolfi et al. (2009)	DBD, 0.002	Air	Kerosene	0.074	4–12	25.0–88.0
Abbas et al. (2020)	DDBD, 40 kV	Air	Naphthalene	0.1	30	96.32
Abbas et al. (2020)	DDBD, 40 kV	Air	Phenanthrene	0.1	30	89.08
Abbas et al. (2020)	DDBD, 40 kV	Air	Pyrene	0.1	30	88.59
Geng et al. (2015)	PDP, 19 kV	Air	Pyrene	0.1–0.3	60	66.7–87.9
Mu et al. (2016)	DBD, 33.8 kV	Air	Pyrene	0.1–0.3	60	~38–66.6
Wang et al. (2016)	PDP, 16.5 kV	Air	Pyrene	0.1–0.3	60	42.1–56.9
Liu et al. (2022c)	DBD, 24 kV	N_2+O_2	Pyrene	0.025–0.2	6	~94–38
Liu et al. (2022c)	DBD, 24 kV	N_2+O_2	Pyrene	0.1	1–10	~25.5–72
Liu et al. (2022c)	DBD + CeO_2 catalyst, 24 kV	N_2+O_2	Pyrene	0.1	1–10	~55–88
Liu et al. (2022c)	DBD + TiO_2 catalyst, 24 kV	N_2+O_2	Pyrene	0.1	1–10	~66–88

1 Thermal plasma blasting + Fenton reagent H_2O_2.

remediation when the soil was contaminated with 5 g/kg of diesel fuel. Meanwhile, 74% of the contaminant was removed from the soil at the same 40 min of treatment time when the initial contaminant concentration in the soil was equal to 10 g/kg. Also, researchers performed the soil remediation process from a heavily contaminated oil field. The initial pollutant concentration was equal to approximately 26.4 g/kg. The authors stated that 63.53% and 70.39% of aromatic and saturated hydrocarbons were removed after 40 min of the soil remediation process in the DBD plasma environment.

Wong et al. (2022) performed diesel fuel contaminated clayey zone in situ remediation by synergizing thermal plasma blasting with the Fenton reaction. The initial diesel fuel concentration in the soil was 2 g/kg. The whole pollutant degradation process lasted 48 h. However, the researchers found that rapid diesel degradation occurred in the first 3 h of the remediation process. Meanwhile, the remained remediation time did not increase the pollutant degradation efficiency. Furthermore, the highest diesel degradation efficiency (88.9–98.5%) was achieved using six times plasma blasting with sole H_2O_2 at 10–20 kV.

Zhan et al. (2019) used pulsed corona discharge (PCD) plasma to remediate gasoline-contaminated soil. Researchers evaluated the impact of the initial gasoline concentration and the plasma-forming gas type on the success of the polluted soil remediation process. In the case of initial gasoline concentration, it was determined that 88% of gasoline was degraded after the 60 min remediation process of contaminated soil when the initial gasoline concentration was 2 g/kg. Measured degradation efficiency was approximately 15% higher than at the primary gasoline concentration of 3 g/kg and 33% higher than at the initial pollutant content of 4 g/kg. Moreover, researchers stated that degradation efficiencies of the gasoline were 86%, 84%, 39%, and 23% under air, oxygen, argon, and nitrogen atmospheres, thus indicating that the gasoline degradation efficiency depended on the plasma forming gas type.

Li et al. (2017) performed the gasoline-contaminated soil remediation process using the pulsed corona discharge (PCD) plasma. The influence of the initial pollutant concentration (2.5–10 g/kg) on the soil remediation with the PCD process was analyzed. The evaluation revealed that the degradation efficiency decreased with the increase of initial pollutant concentration. Accordingly, after an hour-long soil remediation process, gasoline was degraded by 81%, 77%, 67%, and 57% from an initial concentration of 2.5 g/kg, 5 g/kg, 7.5 g/kg, and 10 g/kg, respectively.

Zhao et al. (2023) used dielectric barrier discharge (DBD) plasma to remediate gasoline-contaminated soil. The initial concentration of the contaminant varied between 2 and 8 g/kg. Authors stated that 91%, 84%, and 72% of contaminant was degraded within an hour during the remediation of soil contaminated with 2 g/kg, 5 g/kg, and 8 g/kg of gasoline. Also, the researchers evaluated the impact of the atmosphere in which the gasoline (5 g/kg) was degraded. It was observed that after an hour of the remediation process, the gasoline removal rate was equal to 92%, 87%, 59%, and ~100% under an atmosphere of air, O_2, N_2, and Ar, respectively.

Aggelopoulos et al. applied dielectric barrier discharge (DBD) plasma for the remediation of the n-dodecane polluted soil. The researchers pointed out that after a 34-min-long soil treatment process, the removal efficiency of the n-dodecane decreased from ~97% to ~91% as the initial pollutant concentration increased from 0.5 g/kg to 50 g/kg, respectively.

Redolfi et al. (2009) used dielectric barrier discharge (DBD) plasma to remediate the kerosene (0.074 g/kg) contaminated soil. The authors noted that after 4–12 min of the remediation process, 25–88% of the contaminant was remediated from the polluted soil.

Abbas et al. (2020) carried out the remediation of soil contaminated with a mixture of polycyclic aromatic hydrocarbons (naphthalene, phenanthrene and pyrene) using double dielectric barrier discharge (DDBD) plasma technology. The initial concentration of the mix of all three types of PAH in the soil was equal to 0.1 g/kg. It was stated that 96.32%, 89.08%, and 88.59% remediation efficiency was achieved when naphthalene, phenanthrene, and pyrene were remediated with DDBD using air as a carrier gas.

Geng et al. (2015) performed pyrene-contaminated soil remediation

using the net-to-net pulsed discharge plasma (PDP). The initial pyrene concentration in the soil varied between 0.1 and 0.3 g/kg. The researchers found that after an hour of the remediation process, pyrene degradation decreased from 87.9% to 72.1% and 66.7%, with the contaminant concentration increasing from 0.1 g/kg to 0.2 g/kg and 0.3 g/kg, respectively.

Mu et al. (2016) used dielectric barrier discharge (DBD) plasma to remediate soil contaminated with pyrene. It was noticed that the initial pyrene concentration directly affected the degradation efficiency. Accordingly, the degradation efficiency decreased from 66.6% to ~42% and ~38% when the pollutant concentration in the soil increased from 0.1 g/kg to 0.2 g/kg and 0.3 g/kg, respectively.

Wang et al. (2016) applied the seven-needle-to-net pulsed discharge plasma (PDP) to remediate soil contaminated with pyrene. Researchers also investigated the effect of the pyrene content in the soil on the pollutant degradation efficiency. As in the studies mentioned above, the investigation revealed that higher pollutant degradation was obtained under the lower pollutant initial concentration. More precisely, the pyrene degradation efficiency decreased from 56.9% to 52.6% and 42.1% when the initial pyrene content increased from 0.1 g/kg to 0.2 g/kg and 0.3 g/kg, respectively.

Liu et al. (2022c) performed the degradation of a typical pollutant in the soil – pyrene using parallel tubes-array dielectric barrier discharge (DBD) plasma cooperating with a catalyst. The initial pyrene concentration in the soil ranged between 0.05 and 0.2 g/kg. The researchers found that after 6 min of the remediation process, pyrene degradation decreased from ~94% to ~85%, ~55%, ~42% and ~38%, with the contaminant concentration increasing from 0.025 g/kg to 0.05 g/kg, 0.1 g/kg, 0.15 g/kg, and 0.2 g/kg, respectively. Also, the pyrene degradation efficiencies in simulated soil after adding catalysts (CeO_2 and TiO_2) were evaluated. It was noticed that both types of catalysts promoted pyrene degradation efficiency compared to solo plasma remediation. For instance, after 6 min of the soil remediation process, the pyrene degradation efficiency was equal to ~58%, ~78% and ~85% when solo plasma, plasma + CeO_2, and plasma + TiO_2 were applied. Moreover, the degradation efficiency increased with an increased remediation time from 1 to 10 min.

Summarily, the other researchers who applied non-thermal plasma remediated soil polluted with much lower content of petroleum products (0.074–50 g/kg). In most cases, removing petroleum compounds from the soil took a longer time (60 min or more) than applying the thermal plasma method presented in this article (27 min). Thus, the thermal plasma shows higher suitability to remove higher concentrations of petroleum compounds from the soil, in a short period, compared to the non-thermal plasma. Also, the presented thermal plasma technology has the capacity to de-pollute a higher amount of contaminated soil compared to the non-thermal plasma scale. Moreover, since thermal plasma technology can work on a larger scale compared to non-thermal plasma, it is more suitable for application to de-pollute the highly PHCs-polluted soil found in industrial areas, oil product storage areas (e.g., former oil bases), or other highly polluted areas where contaminated soil must immediately be collected and remediated. However, the research of PHCs-diesel contaminated soil de-pollution by thermal plasma technology presented in this article is still in the laboratory exploration stage. Thus, the exact cost at the industrial level and overall economic aspect can not be provided at this stage of technology development.

4. Conclusions

Thermal plasma-based remediation of PHCs–diesel contaminated soil was presented in this experimental study.

The experimental results showed that 99.9% contaminant removal efficiency was received during the PHCs–diesel contaminated soil de-pollution process in the thermal plasma environment regardless of whether water vapor or air was used as a plasma-forming gas.

Furthermore, the soil's contaminant concentration (80–160 g/kg) did not impact the degradation efficiency extent.

Soil surface morphology analysis revealed that soil contamination with PHCs–diesel caused increased soil surface roughness compared to pure soil. However, after the de-pollution process in the water vapor plasma or air plasma environments, the soil surface demonstrated relatively smoothness close to clean soil.

Soil elemental composition evaluation showed that irrespective of the plasma-forming gas type (air or water vapor) soil de-pollution process not only succeeded PHCs–diesel removal from the soil but also caused the decomposition of the natural carbon reserves in the soil.

Thermogravimetric analysis revealed the exact time and temperature of the pure diesel combustion. Such data helped to identify the PHCs–diesel conduct during the combustion process of soil contaminated with different concentrations of the PHCs–diesel.

Also, up to 30.6–51.1 vol% of synthesis gas (H_2+CO) was produced when water vapor plasma was used for the contaminated soil de-pollution process. However, only traces of the synthesis gas were observed when the soil was de-polluted in an air plasma environment.

Further research using different operation parameters (e.g., different amounts of the plasma-forming gas and contaminant) should reveal how the soil remediation process in the thermal plasma environment could be further improved and optimized.

Author contributions

Dovilė Gimžauskaitė: conceptualization, methodology, validation, investigation, writing-original draft, writing-review & editing, visualization. **Andrius Tamošiūnas:** conceptualization, methodology, validation, investigation, writing-original draft, writing-review & editing, project administration. **Mindaugas Aikas:** methodology, investigation. **Rolandas Uscila:** methodology, investigation. All authors read and approved the final manuscript.

Funding

This research received no specific grant from funding agencies in the public, commercial, or not-for-profit sectors.

Declaration of competing interest

The authors declare that they have no known competing financial interests or personal relationships that could have appeared to influence the work reported in this paper.

Data availability

Data will be made available on request.

References

Abbas, Y., Lu, W., Dai, H., Fu, X., Ye, R., Wang, H., 2020. Remediation of polycyclic aromatic hydrocarbons (PAHs) contaminated soil with double dielectric barrier discharge plasma technology: influencing parameters. Chem. Eng. J. 394 https://doi.org/10.1016/j.cej.2020.124858.

Aggelopoulos, C.A., 2022. Recent advances of cold plasma technology for water and soil remediation: a critical review. Chem. Eng. J. https://doi.org/10.1016/j.cej.2021.131657.

Aggelopoulos, C.A., 2016. Atmospheric pressure dielectric barrier discharge for the remediation of soil contaminated by organic pollutants. Int. J. Environ. Sci. Technol. 13, 1731–1740. https://doi.org/10.1007/s13762-016-1009-0.

Ambaye, T.G., Chebbi, A., Formicola, F., Prasad, S., Gomez, F.H., Franzetti, A., Vaccari, M., 2022. Remediation of soil polluted with petroleum hydrocarbons and its reuse for agriculture: recent progress, challenges, and perspectives. Chemosphere. https://doi.org/10.1016/j.chemosphere.2022.133572.

Azhar, U., Ahmad, H., Shafqat, H., Babar, M., Shahzad Munir, H.M., Sagir, M., Arif, M., Hassan, A., Rachmadona, N., Rajendran, S., Mubashir, M., Khoo, K.S., 2022. Remediation techniques for elimination of heavy metal pollutants from soil: a review. Environ. Res. 214 https://doi.org/10.1016/j.envres.2022.113918.

Dai, C., Han, Y., Duan, Y., Lai, X., Fu, R., Liu, S., Leong, K.H., Tu, Y., Zhou, L., 2022. Review on the contamination and remediation of polycyclic aromatic hydrocarbons

(PAHs) in coastal soil and sediments. Environ. Res. https://doi.org/10.1016/j.envres.2021.112423.
Das, N., Bhuyan, B., Pandey, P., 2022. Correlation of soil microbiome with crude oil contamination drives detection of hydrocarbon degrading genes which are independent to quantity and type of contaminants. Environ. Res. 215 https://doi.org/10.1016/j.envres.2022.114185.
FAO, UNEP, 2021. Global Assessment of Soil Pollution- Summary for Policy Makers. Rome. https://doi.org/10.4060/cb4827en.
Geng, C., Wu, C., du, Wang, juan, H., , Yi, wu, C., 2015. Effect of chemical parameters on pyrene degradation in soil in a pulsed discharge plasma system. J. Electrost. 73, 38–42. https://doi.org/10.1016/j.elstat.2014.10.006.
Gimžauskaitė, D., Aikas, M., Tamošiūnas, A., 2022. Recent progress in thermal plasma gasification of liquid and solid wastes. In: Recent Advances in Renewable Energy Technologies. https://doi.org/10.1016/b978-0-12-823532-4.00007-0.
Gimžauskaitė, D., Tamošiūnas, A., Tučkutė, S., Snapkauskienė, V., Aikas, M., Uscila, R., 2020. Treatment of diesel-contaminated soil using thermal water vapor arc plasma. Environ. Sci. Pollut. Control Ser. 27, 43–54. https://doi.org/10.1007/s11356-019-06697-4.
Gkorezis, P., Daghio, M., Franzetti, A., van Hamme, J.D., Sillen, W., Vangronsveld, J., 2016. The interaction between plants and bacteria in the remediation of petroleum hydrocarbons: an environmental perspective. Front. Microbiol. https://doi.org/10.3389/fmicb.2016.01836.
Haider, F.U., Ejaz, M., Cheema, S.A., Khan, M.I., Zhao, B., Liqun, C., Salim, M.A., Naveed, M., Khan, N., Núñez-Delgado, A., Mustafa, A., 2021. Phytotoxicity of petroleum hydrocarbons: sources, impacts and remediation strategies. Environ. Res. 197 https://doi.org/10.1016/j.envres.2021.111031.
Hidalgo, K.J., Teramoto, E.H., Soriano, A.U., Valoni, E., Baessa, M.P., Richnow, H.H., Vogt, C., Chang, H.K., Valéria, M.O., 2020. Taxonomic and functional diversity of the microbiome in a jet fuel contaminated site as revealed by combined application of in situ microcosms with metagenomic analysis. Sci. Total Environ. 708 https://doi.org/10.1016/j.scitotenv.2019.135152.
Judée, F., Simon, S., Bailly, C., Dufour, T., 2018. Plasma-activation of tap water using DBD for agronomy applications: identification and quantification of long lifetime chemical species and production/consumption mechanisms. Water Res. 133, 47–59. https://doi.org/10.1016/j.watres.2017.12.035.
Kapaldo, J., Han, X., Ptasinska, S., 2019. Shielding-gas-controlled atmospheric pressure plasma jets: optical emission, reactive oxygen species, and the effect on cancer cells. Plasma Process. Polym. 16 https://doi.org/10.1002/ppap.201800169.
Lee, D.H., Kim, K.T., Cha, M.S., Song, Y.H., 2010. Effect of excess oxygen in plasma reforming of diesel fuel. Int. J. Hydrogen Energy 35, 4668–4675. https://doi.org/10.1016/j.ijhydene.2010.02.091.
Li, R., Liu, Y., Mu, R., Cheng, W., Ognier, S., 2017. Evaluation of pulsed corona discharge plasma for the treatment of petroleum-contaminated soil. Environ. Sci. Pollut. Control Ser. 24, 1450–1458. https://doi.org/10.1007/s11356-016-7929-x.
Liu, C., Kwon, J.H., Prabhu, S.M., Ha, G.S., Khan, M.A., Park, Y.K., Jeon, B.H., 2022a. Efficiency of diesel-contaminated soil washing with different tween 80 surfactant concentrations, pH, and bentonite ratios. Environ. Res. 214 https://doi.org/10.1016/j.envres.2022.113830.
Liu, F., Zhao, J., Ma, Y., Liu, Z., Xu, Y., Zhang, H., 2022b. Removal of diesel from soil washing effluent by electro-enhanced Fe2+ activated persulfate process. J. Electroanal. Chem. 906 https://doi.org/10.1016/j.jelechem.2021.115995.
Liu, Q., Chen, H., Su, Y., Sun, S., Zhao, C., Zhang, X., Gu, Y., Li, L., 2023. Enhanced crude oil degradation by remodeling of crude oil-contaminated soil microbial community structure using sodium alginate/graphene oxide/Bacillus C5 immobilized pellets. Environ. Res. 223 https://doi.org/10.1016/j.envres.2023.115465.
Liu, Y., Liang, J., Zhou, X., Yuan, H., Li, Y., Chang, D., Yang, K., Yang, D., 2022c. Degradation of persistent organic pollutants in soil by parallel tubes-array dielectric barrier discharge plasma cooperating with catalyst. Chem. Eng. J. 437 https://doi.org/10.1016/j.cej.2022.135089.
Lv, Y., Bao, J., Zhu, L., 2022. A comprehensive review of recent and perspective technologies and challenges for the remediation of oil-contaminated sites. Energy Rep. https://doi.org/10.1016/j.egyr.2022.06.034.
Mambwe, M., Kalebaila, K.K., Johnson, T., 2021. Remediation technologies for oil contaminated soil. Glob. J. Environ. Sci. Manag. 7, 1–20. https://doi.org/10.22034/GJESM.2021.03.07.
Martin, S., Kraaij, G., Ascher, T., Baltzopoulou, P., Karagiannakis, G., Wails, D., Wörner, A., 2015. Direct steam reforming of diesel and diesel-biodiesel blends for distributed hydrogen generation. Int. J. Hydrogen Energy 40, 75–84. https://doi.org/10.1016/j.ijhydene.2014.10.062.
Mu, R., Liu, Y., Li, R., Xue, G., Ognier, S., 2016. Remediation of pyrene-contaminated soil by active species generated from flat-plate dielectric barrier discharge. Chem. Eng. J. 296, 356–365. https://doi.org/10.1016/j.cej.2016.03.106.
Murphy, C.W.M., Davis, G.B., Rayner, J.L., Walsh, T., Bastow, T.P., Butler, A.P., Puzon, G.J., Morgan, M.J., 2022. The role of predicted chemotactic and hydrocarbon degrading taxa in natural source zone depletion at a legacy petroleum hydrocarbon site. J. Hazard Mater. 430 https://doi.org/10.1016/j.jhazmat.2022.128482.
Ossai, I.C., Ahmed, A., Hassan, A., Hamid, F.S., 2020. Remediation of soil and water contaminated with petroleum hydrocarbon: a review. Environ. Technol. Innov. https://doi.org/10.1016/j.eti.2019.100526.
Peters, R., Pasel, J., Samsun, R.C., Scharf, F., Tschauder, A., Stolten, D., 2018. Heat exchanger design for autothermal reforming of diesel. Int. J. Hydrogen Energy 43, 11830–11846. https://doi.org/10.1016/j.ijhydene.2018.03.085.
Piqueras, P., García, A., Monsalve-Serrano, J., Ruiz, M.J., 2019. Performance of a diesel oxidation catalyst under diesel-gasoline reactivity controlled compression ignition combustion conditions. Energy Convers. Manag. 196, 18–31. https://doi.org/10.1016/j.enconman.2019.05.111.
Priyadarshini, I., Chattopadhyay, P., 2022. Remediation of Diesel-contaminated soil using zero-valent nano-nickel and zero-valent nano copper particles-stabilized Tween 80 surfactant foam. Mater. Today: Proc. https://doi.org/10.1016/j.matpr.2022.11.428.
Rahman, Z., Rahman, H., Rahman, A., 2015. Classification and generation of atmospheric pressure plasma and its principle applications. Int. J. Math. Phys. Sci. Res. 2, 127–146.
Redolfi, M., Makhloufi, C., Ognier, S., Cavadias, S., Tzovolou, D., Tsakiroglou, Ch, 2009. Kerosene contaminated soil removal by non-thermal atmospheric plasma discharge. High Temp. Mater. Process. 13, 427–437. https://doi.org/10.1615/HighTempMatProc.v13.i3-4.140.
Sanito, R.C., You, S.J., Wang, Y.F., 2022. Degradation of contaminants in plasma technology: an overview. J. Hazard Mater. https://doi.org/10.1016/j.jhazmat.2021.127390.
Sanjaya, E., Abbas, A., 2023. Plasma gasification as an alternative energy-from-waste (EFW) technology for the circular economy: an environmental review. Resour. Conserv. Recycl. 189, 106730 https://doi.org/10.1016/j.resconrec.2022.106730.
Shang, Z., Xu, P., Ke, Z., Yao, M., Li, X., 2023. Diesel removal and recovery from heavily diesel-contaminated soil based on three-liquid-phase equilibria of diesel + 2-butyloxyethanol + water. J. Hazard Mater. 442 https://doi.org/10.1016/j.jhazmat.2022.130061.
Shen, J., Zhang, H., Xu, Z., Zhang, Z., Cheng, C., Ni, G., Lan, Y., Meng, Y., Xia, W., Chu, P. K., 2019. Preferential production of reactive species and bactericidal efficacy of gas-liquid plasma discharge. Chem. Eng. J. 362, 402–412. https://doi.org/10.1016/j.cej.2019.01.018.
Snellings, R., Mertens, G., Elsen, J., 2012. Supplementary Cementitious Materials. Rev Mineral Geochem. https://doi.org/10.2138/rmg.2012.74.6.
Song, Y., Han, K., Wang, D. yang, 2020. Thermodynamic analysis of fossil fuels reforming for fuel cell application. Int. J. Hydrogen Energy 45, 20232–20239. https://doi.org/10.1016/j.ijhydene.2019.11.175.
Topolovec, B., Škoro, N., Puač, N., Petrovic, M., 2022. Pathways of organic micropollutants degradation in atmospheric pressure plasma processing – a review. Chemosphere. https://doi.org/10.1016/j.chemosphere.2022.133606.
Wang, H., Zhou, G., Guo, H., Ge, Z., Yi, C., 2016. Organic compounds removal in soil in a seven-needle-to-net pulsed discharge plasma system. J. Electrost. 80, 69–75. https://doi.org/10.1016/j.elstat.2016.02.002.
Wang, W., Snoeckx, R., Zhang, X., Cha, M.S., Bogaerts, A., 2018. Modeling plasma-based CO2 and CH4 conversion in mixtures with N2, O2, and H2O: the bigger plasma chemistry picture. J. Phys. Chem. C 122, 8704–8723. https://doi.org/10.1021/acs.jpcc.7b10619.
Wong, K.T., Jang, S.B., Choong, C.E., Kang, C. won, Lee, G.C., Song, J.Y., Yoon, Y., Jang, M., 2022. In situ Fenton remediation for diesel contaminated clayey zone assisted by thermal plasma blasting: synergism and cost estimation. Chemosphere 286. https://doi.org/10.1016/j.chemosphere.2021.131574.
Zhan, J., Zhang, A., Héroux, P., Li, X., Li, Z., Zhao, J., Guo, Y., Liu, Y., 2019. Gasoline degradation and nitrogen fixation in soil by pulsed corona discharge plasma. Sci. Total Environ. 661, 266–275. https://doi.org/10.1016/j.scitotenv.2019.01.183.
Zhao, J., Zhang, A., Héroux, P., Sun, Z., Liu, Y., 2021. Remediation of diesel fuel polluted soil using dielectric barrier discharge plasma. Chem. Eng. J. 417 https://doi.org/10.1016/j.cej.2020.128143.
Zhao, J., Zhang, H., Zhan, J., Zhang, A., Zhu, L., Sun, Z., Liu, Y., 2023. Contrastive study on organic contaminated soils remediated using dielectric barrier discharge (DBD) plasma. In: Sep Purif Technol, vol. 306. https://doi.org/10.1016/j.seppur.2022.122576.
Zheng, J., Yang, R., Xie, L., Jianglan, Q., Yang, L., Xingguo, L., 2010. Plasma-assisted approaches in inorganic nanostructure fabrication. Adv. Mater. https://doi.org/10.1002/adma.200903147.